

Evidence for s–d Hybridization in Au₃₈ Clusters

Yaroslav B. Losovyj,[†] Shao-Chun Li,[‡] Natalia Lozova,[†] Khabibulakh Katsiev,[§] Daniel Stellwagen,^{||} Ulrike Diebold,^{‡,⊥} Lingmei Kong,[#] and Challa S. S. R. Kumar^{*,†,▽}

[†]Center for Advanced Microstructures and Devices, Louisiana State University, Baton Rouge, Louisiana 70806, United States

[‡]Department of Physics, Tulane University, New Orleans, Louisiana 70188, United States

[§]Department of Chemistry, Texas A&M University, College Station, Texas 77842, United States

^{||}Utrecht University, P.O. Box 80083, 3508 TC Utrecht, The Netherlands

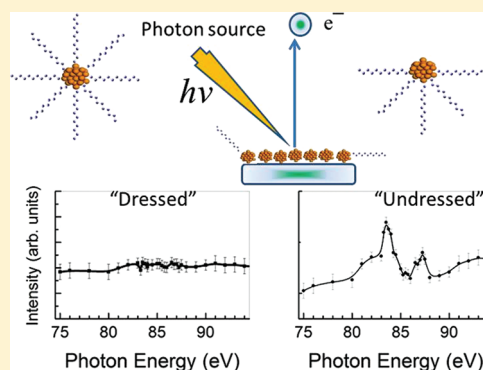
[⊥]Vienna University of Technology, Institute of Applied Physics, E134, Wiedner Hauptstr. 8-10, 1040 Vienna, Austria

[#]Nebraska Center for Materials and Nanoscience, Department of Physics and Astronomy, Theodore Jorgensen Hall, University of Nebraska—Lincoln, 855 North 16th Street, Lincoln, Nebraska 68588-0299, United States

[▽]Center for Atomic-level Catalyst Design (CALC-D), 110 Chemical Engineering, South Stadium Road, Baton Rouge, Louisiana 70803

S Supporting Information

ABSTRACT: Resonant enhancement is seen in some gold clusters at the gold 4f_{7/2} and 4f_{5/2} threshold, indicative of an f to d transition. The existence of such resonance is generally not observed in ultrasmall Au nanoclusters because this resonant transition is forbidden in atomic gold, as gold represents a filled 5d¹⁰6s¹ system. Here we report, for the first time, the presence of a strong resonant enhancement in photoemission at the 4f_{7/2} threshold and a weaker resonant enhancement at the 4f_{5/2} threshold, in the open (undressed) Au₃₈ cluster system, indicating not only an f to d Coster–Kronig resonance but also s–d hybridization, much like what is observed in gold films. This f to d Coster–Kronig photoemission resonance is not observed in the “undressed” thiol-terminated gold clusters characteristic of far more localized orbitals. These results indicate that the unusual catalytic properties of ultrasmall gold nanoclusters such as Au₃₈ are not a result of localized orbitals, which is the case in a molecular system.



INTRODUCTION

Atomically precise methods to prepare and characterize catalysts under vacuum conditions are relatively well developed.¹ However, their practical utility is negligible due to the inability to obtain sufficient quantities for practical catalysis. While chemical methods to synthesize large quantities of catalysts are well developed, there is an unfulfilled need for developing chemical methods for synthesizing atomically precise catalysts.² Through recent computational studies, the presence of electronic quantum size effects in structurally well-characterized ligand-protected gold clusters with diameters between 1.2 and 2.4 nm has been demonstrated.³ It has been shown, albeit theoretically, that the magnitude of the HOMO–LUMO energy gap plays a crucial role in binding oxygen to the nanocatalyst in an activated form. However, the electronic structure of such wet-chemically synthesized, atomically precise practical catalysts has never been correlated with their catalytic activity and selectivity. One of the grand science challenges is to understand how remarkable properties of matter emerge from complex correlations of the atomic or electronic constituents and how we can control these properties.⁴ If we can learn to direct and control material processes at the level of electrons,

where the laws of quantum mechanics rule, it should pave the way for an entirely new generation of catalysts that offer high efficiency and selectivity in a number of energy efficient processes. By advancing tools to correlate the fundamental electronic structure of atomically precise practical catalysts, made using wet-chemical methods, with their catalysis, one could design better practical catalysts.

Major differences in catalytic properties are documented for gold as a thin film or a nanoparticle,^{5–7} a gold nanoparticle on an oxide substrate,^{7,8} or a free gold cluster in vacuum.⁹ Yet, in investigating gold clusters,^{3,6,7} the all-important joint density of occupied and unoccupied states in the vicinity of the Fermi level is rarely considered.³ One key issue is whether the gold cluster should be treated as a molecule or as a metallic cluster: is the catalytic reaction chemistry mediated by localized or delocalized states? One cannot simply measure the electronic structure of an ultrasmall gold cluster and determine the electronic state localization, as ultrasmall clusters are not

Received: February 1, 2012

Revised: February 7, 2012

Published: February 8, 2012



amenable to band dispersion measurements (changes in binding energy with changes in wave vector). Band width and orbital delocalization can, however, be investigated through resonant photoemission, especially in the case of gold. Gold is a filled $5d^{10}6s^1$ system, hence a $4f$ to $5d$ resonant transition is forbidden unless there is significant bandwidth and d - s - p hybridization. The existence of a strong photoemission resonant enhancement at the $4f_{7/2}$ threshold thus allows the experimentalist to probe the s - p - d hybridization associated with a metallic-like band structure, even in a gold nanocluster. Here we report our findings into probing the s - p - d hybridization in $Au_{38}(SR)_{24}$ clusters.

■ EXPERIMENTAL

Chemicals: RES. The following chemicals used in this work are of highest purity, which were obtained from Sigma Aldrich and used as received. Tetrachloroauric(III) acid (99.99%); L-Glutathione reduced (>98%); Sodium borohydride (99.99%); Acetone (HPLC-grade); Ethanol (HPLC-grade); Methanol (anhydrous); Toluene (HPLC-grade); 1-Dodecanethiol (>98%).

Synthesis of Dodecanethiol-stabilized $Au_{38}(SR)_{24}$ Clusters. In a typical process, two solutions of 0.5 g (1.25 mmol) $HAuCl_4 \cdot 3H_2O$ dissolved in 80 mL MeOH and 1.55 g (5 mmol) glutathione dissolved in 40 mL nanopure water were mixed, upon which a white suspension ($Au(I)SG$ polymer) formed instantly. The white suspension was cooled to $0^\circ C$, and a cold $NaBH_4$ solution (0.47 g, 12.5 mmol in 24 mL nanopure water) was added under vigorous stirring. The black suspension was kept at $0^\circ C$ for 1 hr, after which the reaction was stopped. The black product (a mixture of $Aun(SG)_m$ clusters) was isolated by centrifugation and washed with 100 mL MeOH. This black product was then dissolved in 12 mL nanopure water and transferred to a reflux setup. Acetone (15 mL) and 20 mL dodecane thiol were added to the solution, yielding a two-phase system in which the black aqueous layer was topped by the transparent thiol layer. The mixture was heated to reaction temperature and left overnight (16 h) while stirring. The reaction mixture was transferred to a separating funnel and the aqueous phase was removed. The target product was precipitated from the remaining solution by adding a non-solvent, and washed several times with copious amounts of EtOH and acetone to remove byproducts and excess free thiol. The $Au_{38}(SR)_{24}$ product was isolated from the remaining fraction by extraction with toluene. The pitch black toluene solution was centrifuged (5000 rpm, 5 min) to remove byproducts. The $Au_{38}(SR)_{24}$ containing supernatant was collected and concentrated. The $Au_{38}(SR)_{24}$ clusters were further purified by a second extraction with a toluene/acetone mixture in order to precipitate byproducts (larger $Aun(SR)_m$ clusters). The concentration of the gold in toluene was found to be 3–4 mg/mL. This was further diluted for photoelectron spectroscopy measurements. The black toluene/acetone solution was collected and the acetone evaporated. The remaining solution was again centrifuged (5000 rpm, 15 min) to obtain pure and monodisperse Au_{38} clusters.

Characterization. Matrix assisted laser desorption/ionization (MALDI) mass spectrometry was performed with a PerSeptive-Biosystems Voyager DE super-STR time-of-flight (TOF) spectrometer at LSU's chemistry department. Trans-2-[3-(4-tert-butylphenyl)-2-methyl-2-propenylidene]-malononitrile (DCTB) was used as the matrix for MALDI. 1 mg of matrix and 0.1 mg of stock solution (1 mg/mL) were

mixed in either 100 μL CH_2Cl_2 or 100 μL toluene. A 10 μL portion was applied to the steel sample plate and then air dried. UV-vis absorption spectra of toluene solution of the samples were measured at LSU's Chemistry Department. Gold L3-edge XAS measurements were performed at the WDCM (wiggler double crystal monochromator) beam line at CAMD. The $Au_{38}(SR)_{24}$ solution was concentrated and added dropwise to Kapton tape. Approximately 200 mg of gold clusters was added to a 1 cm^2 area of Kapton. This sample was compared with gold(I)sulfide, gold foil and larger gold colloids (3 nm). The XANES spectra were recorded in transmission mode and averaged over multiple scans. TEM images were recorded at University of Texas in Arlington (UTA) using Hitachi H-9500 high-resolution TEM.

Photoemission Experiments. The angle-resolved photoemission experiments were performed using the 3 m toroidal grating monochromator (3 m TGM) beam line at CAMD in a UHV chamber previously described.¹⁰ The light incident angle of 45° (s - p -polarized light, or with more the vector potential \vec{A} in plane of the surface) in respect to the sample surface normal, making use of the highly linearly polarized light from the synchrotron, as is now commonly done.¹¹ The high resolution ultra violet photoemission spectroscopy (UPS) was done using the 3 m normal incident grating monochromator (3 m NIM) beam line at CAMD and a Scienta 200 hemispherical electron analyzer and collecting the photo-electrons emitted normal to the surface normal. The ultimate combined resolution of that system is better than 10 meV as inferred from widths of the photoionization spectra for the Ar $3p_{1/2}$ (15.8 eV) and $3p_{3/2}$ (15.9 eV). The resolution was set to 50 meV. All binding energies are referenced with respect to the Fermi edge of tantalum foil in electrical contact with the sample and measurements were carried out at ambient temperatures.

■ RESULTS AND DISCUSSION

The $Au_{38}(SR)_{24}$ clusters, stabilized by dodecane thiol and other thiols, were synthesized using protocols modified in our laboratory and were characterized in multiple ways, including MALDI, UV-vis, and XAS (see Supporting Information).¹² We have further analyzed these clusters using scanning tunneling microscopy (STM). The STM image indicated that the size distribution of the clusters is quite uniform as seen in Figure 1, and this assessment is also supported by transmission electron microscopy (TEM, shown in Supporting Information). The STM line profile in Figure 1(c) indicates that the clusters order on the SiO_2 surface with a 2.5 nm spacing between the clusters. The clusters appear well-organized with a clear short-range hexagonal ordering, different from what was observed for Au_{55} clusters on HOPG with STM.¹³

Photon energy dependent (resonant) photoemission spectroscopy measurements (see Figure 2) were conducted using plane-polarized synchrotron radiation dispersed by a 3 m toroidal grating monochromator^{10,14} at the Center for Advanced Microstructures and Devices (CAMD).¹⁵ The measurements were performed in a UHV chamber employing a hemispherical electron analyzer with an angular acceptance of $+1^\circ$, as described elsewhere.^{10,14} The combined resolution of the electron energy analyzer and the monochromator was 120–150 meV. Samples were typically prepared by depositing the diluted solution onto a Si(111) sample with a native SiO_2 layer. Valence band spectra as a function of photon energy were collected along the surface normal to preserve the valence band photoemission spectra of these gold clusters and do not exhibit

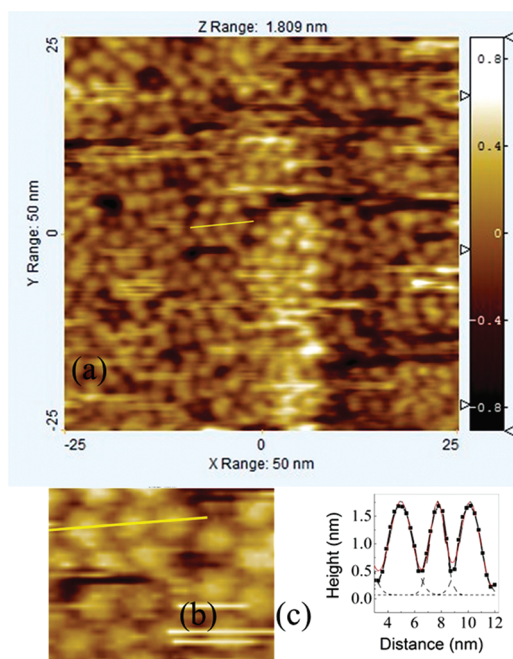


Figure 1. (a) Scanning tunneling microscopy ($50 \times 50 \text{ nm}^2$) image of gold dodecane thiol-stabilized $\text{Au}_{38}(\text{SR})_{24}$ clusters deposited from solution on a Si(111) sample with a SiO_2 native oxide surface (just as from the box, washed with ethanol and distilled water) and (b) small-scale part of image $10.2 \times 13.5 \text{ nm}^2$. (c) Line profile taken at the position indicated with the yellow line in (a,b) indicates that the clusters are $\sim 1.8 \text{ nm}$ in height with a spacing of 2.5 nm between them.

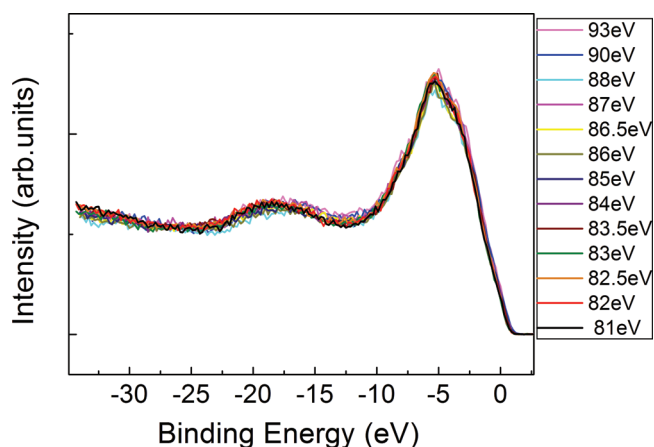


Figure 2. Valence band photoemission spectra, as a function of photon energy, of $\text{Au}_{38}(\text{SR})_{24}$ clusters deposited from solution on Si(111) with a native SiO_2 oxide. The spectra have been aligned to the Fermi level of gold and normalized to photon flux. Note the absence of any significant variations in the spectra with photon energies.

the typical metallic 5d band density of states with two representative gold features located at about $\sim 3 \text{ eV}$ and ~ 6 to 7 eV binding energy. After a sputtering (500 eV , $1\text{--}3 \mu\text{A}$) and annealing treatment to remove (undress) the dodecane thiol groups that dress the Au_{38} clusters, the valence band photoemission spectra resemble that of metallic gold (Figure 3). There are some differences in the relative binding energies; both the Au 4f core levels and the valence band states are shifted to higher binding energies relative to the bulk gold film (Figure 3). Both the finite size of Au_{38} and the insulating character of the SiO_2 substrate could contribute to a decreased

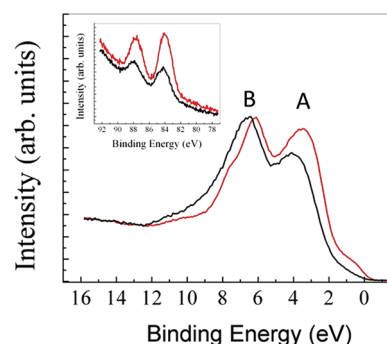


Figure 3. Valence band photoemission spectrum of gold dodecane thiol-stabilized $\text{Au}_{38}(\text{SR})_{24}$ clusters deposited from solution onto the SiO_2 native oxide surface prepared on Si(111), after sputtering to remove the alkyl thiol ligands (black). The spectrum is compared to a micrometer thick (111) textured gold film (red). The photon energy is 73 eV . The inset shows the 4f core level region for photon energy of 125 eV .

screening and to effectively greater photoemission binding energies. The low density of states at the Fermi level for the undressed clusters is consistent with a decrease in metallicity relative to the bulk gold film. Au clusters of only a few atoms on silica are known not to be metallic,¹⁶ and such clusters would have a negligible density of states at the Fermi level. Even Au_{38} , as long as it remains in a high symmetry geometric arrangement, should retain a significant gap between the lowest unoccupied molecular orbital (LUMO) and the highest occupied molecular orbital (HOMO).¹⁷

Yet free Cu,¹⁸ Ag,^{19,20} and Au²¹ clusters are believed to exhibit strong s–d hybridization, and the undressed Au_{38} clusters studied here are unlikely to adopt a high symmetry geometry once some or most of the dodecane thiol ligands are removed. In Figure 4, the resonant enhancement of the valence

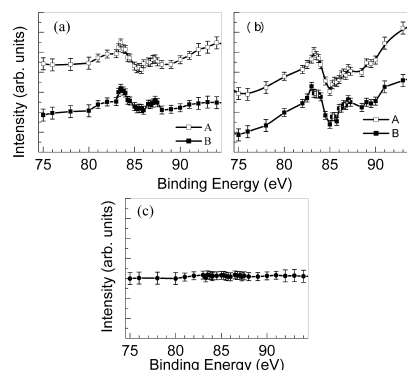


Figure 4. Photoemission intensities at binding energies of $\sim 3 \text{ eV}$ (A) and 6.5 eV (B) (see Figure 3) vs photon energies for (a) gold dodecane thiol-stabilized $\text{Au}_{38}(\text{SR})_{24}$ clusters deposited from solution on the SiO_2 native oxide surface of Si(111), after sputtering to remove the alkyl thiol ligands, and (b) thick (111) textured gold film. (c) Photoemission intensities at binding energy of $\sim 6.5 \text{ eV}$ (B) vs photon energies for ligand protected $\text{Au}_{38}(\text{SR})_{24}$ clusters.

band photoemission spectra has been plotted at the gold $4f_{7/2}$ and $4f_{5/2}$ thresholds. These intensity increases in the photoemission spectra, at roughly the gold $4f_{7/2}$ and $4f_{5/2}$ core binding energies, are indicative of f to d transitions. This can only occur if there is, in fact, s–d hybridization leading to partial, rather than complete, occupancy of the valence 5d bands. In fact these photoemission resonances are very similar

to those seen in metallic gold, where s – d hybridization is both expected and observed.

Results from recent studies show the stability of Au clusters, grown on amorphous carbon, against agglomeration even after exposure to high ionization.²² On the basis of these results and also our own data as discussed below, we believe that the active adsorption surface of most of the clusters remains unchanged at least for several sputtering cycles with 500 eV and 1–2 μ A ion current at annealing temperatures of 200 °C. This is the same procedure we used initially to remove some of the ligands to open the active adsorption surface on the original clusters. Figure 5a shows two typical spectra corresponding to a clean

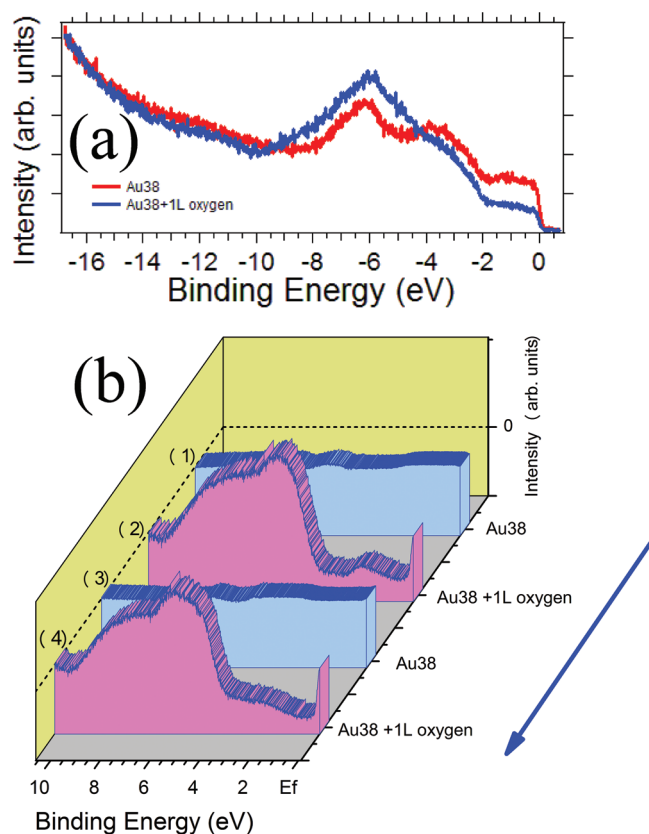


Figure 5. (a) Photoemission spectra ($h\nu = 27.0$ eV) obtained for the clean (marked by red color, see text) Au₃₈ gold nanocluster surface and after oxygen adsorption (blue) normalized to the photon flux. (b) Series of difference photoemission spectra ($h\nu = 21.2$ eV) of the clean (see text) gold Au₃₈ nanoclusters surface (marked 1,3) and after 1 Langmuir of oxygen exposure (marked 2,4) demonstrating cycles of oxygen removal/deposition.

and exposed to oxygen clusters surface. The reproducibility of oxygen adsorption on our Au₃₈ clusters is evident in a series of difference curves in Figure 5b (each difference curve reveals induced features, if applicable, after subtraction of clean cluster spectra). Here we show repeated oxygen adsorption (2,4) and removal by sputtering (1,3) at partly “undressed” Au₃₈ clusters on SiO₂. Similar results are obtained for several cycles. The oxygen exposure is similar in all cases and is 1.0 Langmuir exposure to the supported gold clusters at 300 K, following the gentle sputtering of the nanoclusters to remove oxygen. We believe that not only oxygen-induced features (marked A–D on Figure 5S in the Supporting Information) support our reasoning that the clusters remain unchanged but also a deep

step at the Fermi level is evidence of substantial depletion of that region by oxygen adsorption. The effect of sputtering on the morphology of Au₃₈ ligand-stabilized nanoclusters was further studied with the UHV STM. There is no noticeable change in the Au cluster morphology such as agglomeration of the partially undressed nanoclusters after sputtering (Figure 6S in Supporting Information).

CONCLUSIONS

In conclusion, the existence of 4f threshold photoemission resonances in the partially undressed Au₃₈(SR)₂₄ clusters deposited on the native SiO₂ oxide layer demonstrates that noble metal clusters, even of ultrasmall size, will exhibit s – d hybridization. Our experimental results indeed support the predictions from density functional theory.^{10,20,21} The photoemission resonant enhancement of the valence band photoemission spectra at the gold 4f_{7/2} and 4f_{5/2} thresholds is indicative of f to d transitions. Such transitions are allowed only if s – d hybridization is present. In ultrasmall gold clusters with highly localized orbitals, such as the clusters completely dressed with thiol groups, these photoemission resonances are not seen, in agreement with a more localized orbital nature in these clusters. The similarities between the Au₃₈ clusters on SiO₂ and pure gold suggest that the s – d hybridization in Au₃₈ is nearly as extensive as in metallic gold.

ASSOCIATED CONTENT

Supporting Information

Experimental methods and material characterization, including UV–vis, MALDI, TEM, XAS, and photoemission. This material is available free of charge via the Internet at <http://pubs.acs.org>.

AUTHOR INFORMATION

Corresponding Author

*E-mail: ckumar1@lsu.edu. Tel.: (225)-578-9320.

Notes

The authors declare no competing financial interest.

ACKNOWLEDGMENTS

This material is based upon work supported as part of the Center for Atomic Level Catalyst Design, an Energy Frontier Research Center funded by the U.S. Department of Energy, Office of Science, Office of Basic Energy Sciences under Award Number DE-SC0001058. Funding from the Center for Atomic-Level Catalyst Design (CALC-D) is gratefully acknowledged. We would like to thank Prof. P. Dowben for valuable discussions.

REFERENCES

- (1) Valden, M.; Lai, X.; Goodman, D. W. *Science* **1998**, *281*, 1647.
- (2) (a) Jin, R. *Nanoscale* **2010**, *2* (3), 343–362. (b) Jin, R. *Nanotechnol. Rev.* **2012**, *1*, 31–56.
- (3) Lopez-Acevedo, O.; Kacprzak, K. A.; Akola, J.; Häkkinen, H. *Nature Chem.* **2010**, *2*, 329–334.
- (4) *Directing Matter and Energy: Five Challenges for Science and the Imagination, A report from the basic energy sciences advisory committee*; DOE: USA, 2007.
- (5) (a) Meier, D. C.; Bukhtiyarov, V.; Goodman, D. W. *J. Phys. Chem. B* **2003**, *107*, 12668. (b) Gottfried, J. M.; Schmidt, K. J.; Schroeder, S. L. M.; Christmann, K. *Surf. Sci.* **2003**, *536*, 206. (c) Jugnet, N.; Cadete Santos Aires, F. J.; Deranlot, C.; Piccolo, L.; Bertolini, J. C. *Surf. Sci.* **2002**, *521*, L639.

- (6) (a) Zhu, Y.; Qian, H. F.; Drake, B. A.; Jin, R. *Angew. Chem., Int. Ed.* **2010**, *49*, 1295. (b) Zhu, Y.; Qian, H. F.; Zhu, M.; Jin, R. *Adv. Mater.* **2010**, *22*, 1–6.
- (7) (a) Longo, A.; Liotta, L. F.; Di Carlo, G.; Giannici, F.; Venezia, A. M.; Martorana, A. *Chem. Mater.* **2010**, *22*, 3952. (b) Brown, M. A.; Carrasco, E.; Sterrer, M.; Freund, H. J. *J. Am. Chem. Soc.* **2010**, *132*, 4064. (c) Liu, Z.-P.; Hu, P. *J. Am. Chem. Soc.* **2002**, *124*, 14770.
- (8) (a) Stolicic, D.; Fischer, M.; Ganteför, G.; Dok Kim, Y.; Sun, Q.; Jena, P. *J. Am. Chem. Soc.* **2003**, *125*, 2848. (b) Wallace, W. T.; Whetten, R. L. *J. Am. Chem. Soc.* **2002**, *124*, 7499.
- (9) (a) Meyer, R.; Lemire, C.; Shaikhutdinov, S. K.; Freund, H. J. *Gold Bull.* **2004**, *37*, 72. (b) Thompson, D. T. *Appl. Catal., A* **2003**, *243*, 201.
- (10) Dowben, P. A.; LaGrafte, D.; Onellion, M. *J. Phys.: Condens. Matter* **1989**, *1*, 6571.
- (11) Eberhardt, W.; Plummer, E. W. *Phys. Rev. B* **1980**, *21*, 3245.
- (12) Stellwagen, D.; Weber, A.; Bovenkamp, L. S.; Jin, R.; Bitter, H.; Kumar, C. S. S. R. *RSC Adv.* **2012**, DOI: 10.1039/C2RA00747A.
- (13) Herrmann, M.; Koltun, R.; Kreibitz, U.; Schmid, G.; Güntherodt, G. *Adv. Funct. Mater.* **2001**, *11*, 202.
- (14) Losovyj, Y.; Ketsman, I.; Morikawa, E.; Wang, Z.; Tang, J.; Dowben, P. A. *Nucl. Instrum. Methods Phys. Res., Sect. A* **2007**, *582*, 264.
- (15) Hormes, J.; Scott, J. D.; Suller, V. P. *Synchrotron Radiat. News* **2006**, *19*, 27.
- (16) Cox, D. M.; Eberhardt, W.; Fayet, P.; Fu, Z.; Kessler, B.; Sherwood, R. D.; Sondrick, D.; Kaldor, A. *Z. Phys. D* **1991**, *20*, 385.
- (17) Ji, M.; Gu, X.; Li, X.; Gong, X. G.; Li, J.; Wang, L. S. *Angew. Chem., Int. Ed.* **2005**, *44*, 7119.
- (18) Massobrio, C.; Pasquarello, A.; Car, R. *Phys. Rev. Lett.* **1995**, *75*, 2104.
- (19) Bonacic-Koutecky, V.; Cespiva, L.; Fantucci, P.; Koutecky, J. *J. Chem. Phys.* **1993**, *98*, 7981.
- (20) Lei, Y.; Yong, G. F.; Zhao, Z.; Zeng, J. *J. Nanosci. Nanotechnol.* **2010**, *10*, 5483.
- (21) Häkkinen, H.; Moseler, M.; Landman, U. *Phys. Rev. Lett.* **2002**, *89*, 033401.
- (22) Visikovskiy, A.; Matsumoto, H.; Mitsuhashi, K.; Nakada, T.; Akita, T.; Kido, Y. *Phys. Rev. B* **2011**, *83*, 165428.